RSC Advances

ROYAL SOCIETY OF CHEMISTRY

www.rsc.org/advances

Journal Name

RSCPublishing

ARTICLE

Hydrogen Physisorption in Ionic Solid Compounds with Exposed Metal Cations at Room Temperature

Cite this: DOI: 10.1039/x0xx00000x

Kapil Pareek, [a] Qingfan Zhang, [b] Rupesh Rohan, [a] Zhang Yunfeng [a] and Hansong Cheng [a,b],

Received 00th January 2012,
Accepted 00th January 2012

DOI: 10.1039/x0xx00000x

www.rsc.org/

Phenol and phloroglucinol based organo-magnesium ionic solid compounds were synthesized for room temperature hydrogen storage via physisorption. These materials contain magnesium dications balanced with highly charge-delocalized anionic species, making the cations highly exposed with relatively weak electrostatic interactions with the anions and thus facilitating the interaction with molecular hydrogen. It was found that the driving force for the hydrogen physisorption in these materials is largely electrostatic with the σ-electrons of hydrogen partially polarized by the cationic charges. The synthesized amorphous complexes exhibit moderate surface areas up to 165 m^2/g and 115 m^2/g with the maximum excess hydrogen sorption capacities of 0.22 wt% and 0.8 wt%, respectively, at 298K and 100 atm. Adsorption isotherms were then taken at 323K, 298K and 273K, yielding the low coverage isosteric heats of adsorption of 7.2 kJ/mol and 12 kJ/mol, respectively, for the ionic solid complexes.

Introduction

The steady decrease of fossil fuels has created a tremendous demand for renewable energies and for higher energy efficiencies, which has stimulated worldwide efforts to develop alternative fuels and technologies for more efficient use of energies. [1] Hydrogen technologies play a vital role in the transition of carbon-based energy economy to renewable-based pollution free economy. [2] Nevertheless, the lack of safe and effective storage technologies severely limits hydrogen to be broadly utilized in the market place. Numerous materials have been investigated in recent years for hydrogen storage via chemisorption or physisorption. [3-5] Hydrogen physisorption would possess obvious advantages over chemisorption if high storage capacity at a near ambient temperature could be achieved due to the excellent operability using the mature pressure swing adsorption (PSA) technology. [3] In comparison, hydrogen chemisorption relies on temperature to control the hydrogen release with a longer response time and a lower efficiency. [6, 7] Hydrogen physisorption at near ambient temperatures has long been considered as a grand challenge, stemming from the difficulty to polarize the molecules. Indeed, most of the physisorption materials exhibit significant hydrogen uptake only at cryogenic temperatures. [3, 8-13]

High hydrogen uptake at near ambient temperatures can be achieved by polarizing hydrogen molecules to induce a stronger interaction than the van der Waals force, as demonstrated in materials with active cationic or anionic sites.[14-17] In the case with active anions, such as partially fluorinated graphite, a significant host-H_2 interaction resulting from partial charge transfer from an anion to the empty σ *-orbital of H_2 gives rise to appreciable hydrogen uptake at room temperature.[18] In the case with active cations, such as metal organic framework (MOF) compounds with exposed metal sites[19] and metal hydrazide gel complexes, stronger host-H_2 interaction than van der Waals forces has been demonstrated.[15-17, 20-22]

In general, three strategies have been employed to synthesize materials with exposed metal sites. [16] The most common approach is to remove metal bonded solvent molecules under the conditions of elevated temperatures and high vacuum as demonstrated in the synthesis of several open metal site MOF materials.[15, 16, 23-25] The second approach is to incorporate coordinatively unsaturated metal centers in organic linkers via either pre or post-modification routes. The exposed metal centers produced in this way would not be part of main backbone of the framework.[16, 17, 26] In the third approach, ion exchange and metal impregnation have been employed to produce exposed metal sites in a framework, as demonstrated in the $Mn_3[(Mn_4Cl)_3(btt)_8(CH_3OH)_{10}]_2$ framework.[27] Although strong hydrogen adsorption in several hypothetical nano-structured carbon materials decorated with metal atoms was predicted theoretically,[28] it has yet to be demonstrated experimentally.

In this paper, we present a novel procedure for design of exposed magnesium metal sites in ionic solid materials (INS) capable of interacting with molecular hydrogen strongly at room temperature via physisorption. The main idea is to make a divalent magnesium ion with two bonds: one bonded covalently with an electron withdrawing organic ligand and another

associated with a bulky anion via electrostatic interaction. With the charge delocalization of the bulky anions, the electrostatic interaction with the divalent magnesium atoms becomes relatively weak, which thus gives rise to exposed magnesium cations in the material. These cations can then serve as the active sites to induce interactions with molecular hydrogen. Base on this consideration, we selected phenoxide and 1,3,5 trioxybenzene as the ligands and tetrafluoroborate anion (BF_4^-) as the bulky anion and synthesized two INS complexes, Ph-INS for phenoxide and Phl-INS for 1,3,5 trioxybenzene $(C_6H_3O_3)^{3-}$. Here, the O-Mg bond formed between magnesium and the ligands is covalent; the interaction between magnesium and BF_4^- is ionic. Technically, it is challenging to synthesize these complexes due to the instability of the reaction intermediates. The difficulty was overcome by selecting appropriate anionic species to pair up with the magnesium dications to form a stable complex. The synthesized Ph-INS and Phl-INS compounds were subsequently characterized prior to the measurement of gas adsorption. The highly exposed cations in these compounds polarize H_2 molecules, leading to an enhanced interaction with the host materials.

Experimental

Materials

Phenol (Sigma Aldrich), phloroglucinol (Sigma Aldrich), tetrahyrofuran (THF) (RCI labscan), methylmagnesium chloride 3.0M in THF (Sigma Aldrich), potassium tetrafluoroborate (Sigma Aldrich). All chemicals were of analytical grade and thus used without further purification except THF. THF was dried over sodium before use.

Synthesis of ionic solid complex

Synthesis of Ph-INS

Phenol (1g, 10.6 mmol) was added to methylmagnesium chloride (10.6 mmol) in THF, and the mixture was stirred at -78°C for ca. 12 h. The observed white precipitate was treated with potassium tetrafluoroborate (1.34g, 10.6 mmol) at 50 °C for 24 h. The reaction was done under argon atmosphere. The precipitated potassium chloride was filtered off and weighed to check for completion of the reaction.[29, 30] The solvent was removed under a reduced pressure with a yield of 85%. FTIR (ATR cm^{-1}): 2927 cm^{-1} (C-H str. aromatic), 1616, 1499 and 1414 cm^{-1} (C=C str. aromatic), 1197, 1161 cm^{-1} (B-F str. BF_4), [31] 1066 cm^{-1} (C-O str.) and 3200-3400 cm^{-1} (adsorbed moisture). CP-MAS ^{13}C NMR: (ppm) 151.95, 128.07, 119.53 and 117.29.

Synthesis of Phl-INS

Phloroglucinol (0.5g, 3.96 mmol) was added to methylmagnesium chloride (11.89 mmol) in THF, and the mixture was stirred at -78 °C for 12 h. The observed yellow precipitate was treated with potassium tetrafluoroborate (1.5g, 11.89 mmol) at 50 °C for 24 h. The reaction was done under argon atmosphere.[29, 32] The precipitated potassium chloride was filtered off and weighed to check for completion of the reaction.[29, 30] The solvents were removed under a reduced pressure by using a rotary evaporator. Final drying was done at 80 °C under vacuum in a tube furnace to produce a yellow powder with a yield of 77 %. FTIR (ATR cm^{-1}): 2918 cm^{-1} (C-H str. aromatic), 1625, 1509 and 1416 cm^{-1} (C=C str. aromatic), 1190, 1157 cm^{-1} (B-F str. BF_4), [31] 1009 cm^{-1} (C-O str.) and 3200-3400 cm^{-1} (adsorbed moisture). CP-MAS ^{13}C NMR: (ppm) 155.45 and 94.75.

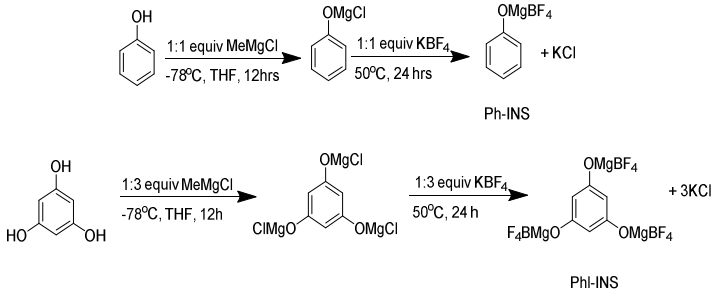

Scheme 1: Synthetic protocol of Ph-INS and Phl-INS materials.

Characterization

Powder X-ray diffraction (XRD) was performed on a D5005 Bruker AXS diffractometer with Cu-Kα radiation (λ = 1.5410) at room temperature. The SEM images were obtained using a scanning electron microscopy (SEM) with QUANTA 200 FEG. Samples were prepared by platinum sputtering under 5×10^{-2} mbar at room temperature (20s, 30mA) with a Baltec SCD050 apparatus. Infrared spectroscopic experiments were conducted on Varian resolutions (version 4.0.5.009). Thermogravimetric analysis was performed on the TA instrument 2960 (DTA-TGA) that covers a temperature range from 25 to 1000 °C. The cross-polarized magic-angle-spinning (CP-MAS) solid state ^{13}C NMR was performed on a Bruker DRX 400 instrument.

High pressure hydrogen gas measurement

Hydrogen adsorption-desorption isotherms were obtained on a computer-controlled commercial Gas Reaction Controller (GRC) manufactured by Advanced Materials Corporation. The GRC instrument, a typical Sieverts apparatus, is based on a volumetric method to determine gas adsorption. The instrument was calibrated rigorously by following the standard procedure recommended by US DOE.[33] The null calibration of an empty sample chamber was done to ensure a zero adsorption baseline at 298K and 77K, respectively. (Fig. S1, Supporting Information) The instrument performance was tested by hydrogen adsorption-desorption isotherms of commercially available adsorbent materials such as basolite A100 and $LaNi_5$ alloy at 77K and 298K, respectively. (Fig. S2 and S3)

The skeleton density of the Ph-INS and Phl-INS complexes was recorded using Quantachrome Ultrapyc 1200e. The instrument was calibrated using spheres with a known volume (0.0898 cc). The volume of an empty sample chamber was obtained by using He gas at room temperature over several running cycles. Around 500 mg of the sample was then loaded into the sample chamber, and the volume of the chamber plus the sample was determined. The skeleton volume of the sample was calculated by subtracting the volume of the chamber plus the sample from the volume of the empty sample chamber. Consequently, the skeleton density of the sample D_{sk} was derived from the following equation:[3]

$$D_{sk}=M/V_{sk} \qquad (1)$$

where M is the sample mass in gram, and V_{sk} is the sample skeleton volume in cm^3 determined by He gas. The value of D_{sk}

was measured 10 times and the average of these D_{sk} data was taken as the final value in order to obtain an accurate skeleton density.

The skeleton densities of the Ph-INS material (1.8 g cm^{-3}) and the Phl-INS material (2.1 g cm^{-3}) were provided to the GRC to obtain an accurate void space volume by subtracting the skeleton volume of the sample from the volume of the sample chamber. With the skeleton density used in the measurement, hydrogen uptake becomes excess adsorption; the compressed hydrogen within the pores is treated as a part of the sample chamber volume and thus the volume of the compressed hydrogen is subtracted.

In a typical adsorption-desorption measurement with GRC, around 500 mg sample was sealed in a sample chamber with a volume of 3 cm^3 under inert atmosphere in a glove box. The skeleton density of the sample was provided to the GRC for accurate calculation of the void space volume by subtracting the skeleton volume of the sample from the volume of the empty sample chamber. High purity hydrogen gas (purity 99.9995%) was used in all the adsorption-desorption measurements. The excess hydrogen uptakes were measured at 273K, 298K and 323K over a pressure range of 0-100 atm.

Enthalpy of adsorption

The enthalpy of the adsorption was calculated using the Clapeyron–Clausius equation by taking the excess hydrogen adsorption data obtained at 323K, 298K and 273K, respectively. The isotherms were fitted using an exponential fit for gas uptake vs. pressure. The exponential equation provides an accurate fit over the pressure up to 100 atm with the goodness of fit (R^2) up to 0.99. The fitted curve was used to obtain the values of P_1 and P_2 at their corresponding amounts of hydrogen adsorbed at T_1 and T_2, respectively. The heat of adsorption was then calculated using Eq. 2. [3]

$$\Delta H_{iso} = -\frac{RT_1T_2}{T_2 - T_1}\ln\frac{P_2}{P_1} \qquad (2)$$

where R is the universal gas constant.

Nitrogen gas adsorption

Nitrogen gas adsorption-desorption isotherms were performed using a Micromeritics ASAP 2020 instrument. In a typical measurement, around 300 mg sample was transferred in a pre-weighted tube under inert atmosphere to prevent exposure of the sample from moisture. The sample was activated under dynamic vacuum at 100 °C. The warm and cold free space corrections were performed for the sample using ultra-high-purity He gas (purity 99.9995%). N_2 adsorption-desorption isotherms were measured in a liquid nitrogen Dewar bath at the maximum pressure range of 1 atm. An oil free pump connected with a turbo-molecular pump was used to prevent the oil contamination during vacuum and feed gas in the activation process and in the isotherm measurements, respectively. The Brunauer-Emmett-Teller (BET) surface area was calculated over the range of relative pressure of 0.05-0.20 bar.

Results and discussions

Table 1. Elemental analysis data of Ph-INS and Phl-INS complex.

Materials		C%	H%	Mg%	B%	F%
Ph-INS	Expected	35.29	2.47	11.90	5.29	37.21
	Found	33.96	2.60	11.10	4.85	35.05
Phl-INS	Expected	15.79	0.66	15.98	7.11	49.95
	Found	16.73	1.50	13.98	6.10	45.85

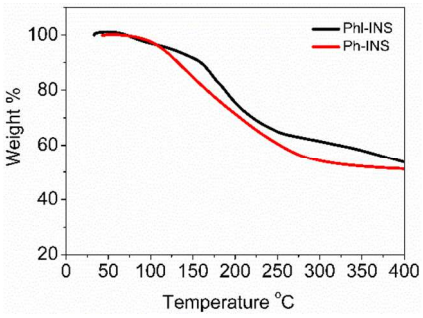

Figure 1. TGA thermograms of Ph-INS and Phl-INS materials under nitrogen atmosphere and 10 °C/min heating rate.

Successful synthesis of the Ph-INS and Phl-INS are supported by the elemental analysis data tabulated in Table 1. The results show a reasonable match between the expected and the detected data. The INS materials contain ca. 5-7% chlorine content, resulting in a modest discrepancy in the expected and the found elemental analysis data. Further purification of these materials are technically challenging due to their high moisture sensitivity and poor solubility in common organic solvents. The thermal stability of Ph-INS and Phl-INS were characterized by TGA thermograms depicted in Fig. 1. Both materials show an initial 5 % weight loss before 120 °C attributed to the adsorbed solvent and moisture. In addition, the steep weight loss observed around 160 °C for Ph-INS and around 176 °C for Phl-INS is attributed to the degradation of tetrafluoroborate anion.[18] The results confirm that the Ph-INS and Phl-INS compounds are both thermally stable at near ambient temperatures.

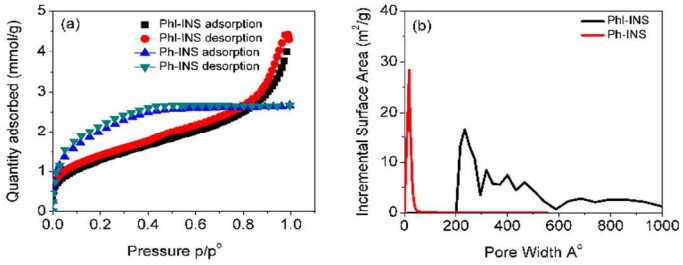

Figure 2. (a) Nitrogen adsorption-desorption isotherms at 77K and 1 atm, and (b) pore size distribution in the Ph-INS and Phl-INS complexes.

Nitrogen adsorption-desorption isotherms at 77K (Fig. 2a) were used to measure the porosity and surface area of the Ph-INS and the Phl-INS complexes. The isotherm for Ph-INS exhibits steep gas uptake in the low pressure range and becomes flat, confirming the mesoporous nature of the material, while the isotherm for Phl-INS displays steep gas uptake at low pressure and capillary condensation at high pressure.[34] The measured

BET surface areas for Ph-INS and Phl-INS are 165 m^2/g and 115 m^2/g, respectively, significantly lower than the reported values of high surface materials, such as MOFs (150-5000 m^2/g) [3] and porous carbons (100-1500 m^2/g),[4] but comparable to the surface areas of metal hydrazide gel materials (90-550 m^2/g).[20-22, 35-37] The pore size distribution (PSD) calculated from the Barrett-Joyner-Halenda (BJH) method for Ph-INS indicates highly uniform porosity with a pore size up to 2.4 nm (Fig. 2b). However, the PSD analysis obtained from a DFT method for Phl-INS gives a wide range of nano-pores (Fig. 2b). In addition, the total pore volume was found to be up to 0.092 cm^3/g for Ph-INS and 0.095 cm^3/g for Phl-INS, respectively. The porosity in the INS materials are extrinsic, arises mainly from inefficient packing of the molecules with a lack of topological self-complementarity.[38]

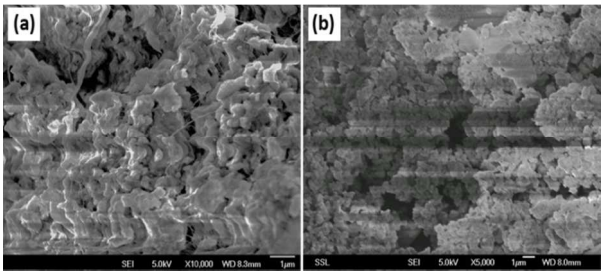

Figure 3. SEM micrographs of (a) Ph-INS and (b) Phl-INS materials.

The mesoporous structure was further investigated by scanning electron microscopy (SEM) shown in Fig. 3. The results suggest that both materials display a series of loosely packed agglomerates.

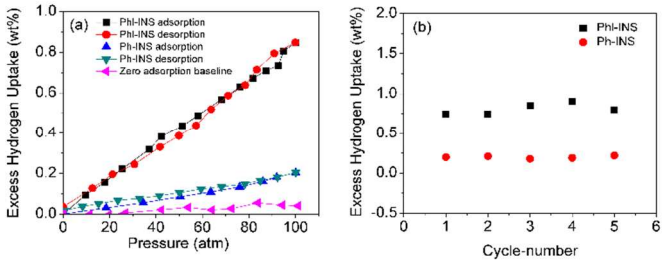

Figure 4. (a) Excess hydrogen uptake at 298K and 100 atm for Ph-INS, Phl-INS and zero adsorption baseline of empty sample holder (b) hydrogen excess capacity at 298K in five fully reversible adsorption-desorption cycles up to 100 atm pressure for Ph-INS (red) and Phl-INS (black).

The measured hydrogen adsorption-desorption isotherms at 298K and 100 atm pressure are shown in Fig. 4a. The isotherms display a linear adsorption curve with the maximum hydrogen storage capacities up to 0.22 wt % for Ph-INS and 0.80 wt% for Phl-INS, respectively. It is important to note that a linear increase of uptake upon gas compression should be ruled out because the apparatus with an empty sample chamber was thoroughly calibrated at 100 atm (Fig. 4a). The zero adsorption base line of the empty sample chamber was then subtracted from the adsorption isotherms of INS materials to minimize error in the measurement. The maximum error in the measurement is up to 0.09 wt% at 298K and 100 atm as suggested by the instrument manufacturer.

The excess of hydrogen uptake at 298K confirms the presence of active metal sites in these INS materials. The charge delocalization of anions weakens the electrostatic interaction with magnesium cations, making the cations more exposed. Such a phenomenon has also been observed in synthesis of single ion polymer electrolytes for Li-ion batteries, in which the weak electrostatic interaction between Li ions and highly charge-delocalized anions gives rise to high Li^+ conductivity.[39] As a consequence, the interaction between H_2 molecules and the highly exposed Mg cations becomes strengthened. The cyclic stability of the Ph-INS and Phl-INS complexes is demonstrated in Fig. 4b through five fully reversible adsorption-desorption cycles at 298K and 100 atm.

The excess hydrogen uptake capacities of the Ph-INS and the Phl-INS complexes at 298K are comparable to the reported values of MOF materials with exposed metal sites tabulated in Table 2, and lower than the Kubas type of metal hydrazide gel materials, such as H_2-Cr-MHz (1.0) (1.65 wt% at 85 atm),[36] vanadium hydride gel C150 (1.17 wt% at 85 atm),[40] and manganese hydride gel B100 (1.06 wt% at 85 atm).[22]

Table 2. Excess hydrogen uptake capacities and heats of hydrogen adsorption of reported exposed metal sites MOF materials.

MOFs	Surface area (m^2/g)	Excess uptake wt% at 298K (pressure in atm)	Heat of adsorption (kJ/mol)	Ref.
SNU-21S	905	0.26 (70)	6.65	41
SNU-21H	695	0.18 (70)	6.09	41
PCN-61	3000	0.667 (90)	6.36	42
PCN-66	4000	0.785 (90)	6.22	42
PCN-68	5109	1.01 (90)	6.09	42
Mn-BTT	2100	0.94 (90)	10.1	15
Cu-BTT	1710	0.46 (90)	9.5	23
MOF-74 (Mg)	1510	0.42 (100)	10.3	43
Cupeip	1560	0.46 (100)	6.63	44
SNU-50	2300	0.399 (100)	7.1	45

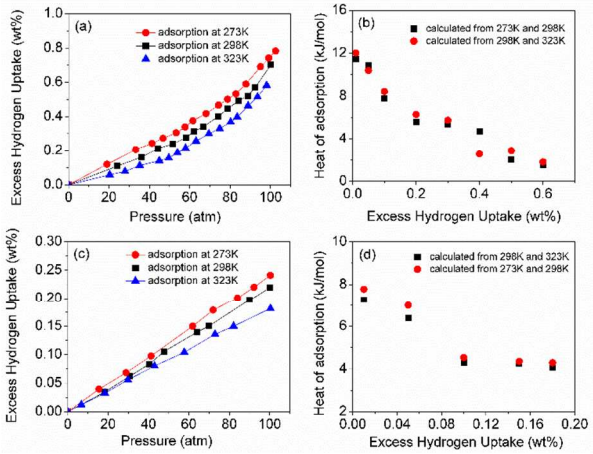

Figure 5. (a) Excess hydrogen adsorption at 273K, 298K and 323K on Phl-INS, (b) the calculated isosteric heat of hydrogen adsorption in Phl-INS, (c) excess hydrogen adsorption at 273K, 298K and 323K on Ph-INS, and (d) the calculated isosteric heat of hydrogen adsorption in Ph-INS.

To describe the adsorption strength quantitatively, the isosteric heats of adsorption were derived from the measured isotherms at 273K, 298K and 323K using the Clausius-Clapeyron equation (Fig.4). The calculated low coverage isosteric heats of adsorption are 7.2 kJ/mol for Ph-INS and 12 kJ/mol for Phl-INS, respectively. The estimated errors in the heat of adsorption calculations are up to 4.02% for Ph-INS and 4.90% for Phl-INS, respectively. The low coverage heats of adsorption of INS materials are comparable to the reported values for high surface area MOF materials with exposed metal sites (Table 2). [3, 15-17, 46, 47]

The comparable heats of adsorption observed in the two ionic solid complexes are attributed to the high exposure of magnesium metal sites to H_2 molecules. Nevertheless, the relatively low specific surface areas of these complexes present a considerable limit to the adsorption capacities. New synthetic strategies need to be designed for preparation of high surface area materials functionalized with exposed magnesium metal sites for high capacity hydrogen storage for practical applications. The results presented in the present study may shed a light on the future development of materials for high capacity hydrogen storage via physisorption at near ambient conditions.

Conclusions

Two ionic solid complexes of Ph-INS and Phl-INS were successfully synthesized for hydrogen physisorption. The materials were characterized via thermal, spectroscopic and surface science techniques. Nitrogen adsorption measurements at 77K yield relatively low BET surface areas of 165 m^2/g for Ph-INS and 115 m^2/g for Phl-INS. At room temperature and 100 atm, the excess hydrogen uptake for Ph-INS is 0.22 wt %, and for Phl-INS it is 0.8 wt%. The maximum hydrogen uptake of these compounds are comparable to what has been reported in several important hydrogen storage materials with active adsorption sites for H_2. The driving force for the strong physisorption arises from the electrostatic interaction between the magnesium dications and the σ-electrons of H_2. Unfortunately, the relatively low surface areas and the lack of complete exposure of the cations may prevent these materials from storing molecular hydrogen with higher capacity at room temperature. Nevertheless, the experimental demonstration of the interactions between an exposed cation and H_2 is important for development of more effective materials to store hydrogen at near ambient temperature via physisorption.

Acknowledgements

The authors gratefully acknowledge support of a Start-up grant from NUS, a POC grant from National Research Foundation of Singapore, a Tier 1 grant from Singapore Ministry of Education (MOE), a DSTA grant and the National Natural Science Foundation of China (No. 21233006). We thank Prof. D. Zhao for stimulating discussions and for his assistance on surface area and pore size measurements.

Notes and references

[a] Department of Chemistry, National University of Singapore, Singapore.117543; E-mail: chmch@nus.edu.sg.

[b] Sustainable Energy Laboratory, China University of Geoscience, Whuan 430074, China.

Electronic Supplementary Information (ESI) available: [Instrument calibration, FTIR, and PXRD].

1. L. Schlapbach and A. Zuttel, *Nature*, 2001, **414**, 353-358.
2. http://www.hydrogen.energy.gov/storage.html, **US Department of Energy, Hydrogen energy**
3. M. P. Suh, H. J. Park, T. K. Prasad and D.-W. Lim, *Chem. Rev.*, 2011, **112**, 782-835.
4. R. Ströbel, J. Garche, P. T. Moseley, L. Jörissen and G. Wolf, *J. Power Sources*, 2006, **159**, 781-801.
5. A. Züttel, P. Sudan, P. Mauron, T. Kiyobayashi, C. Emmenegger and L. Schlapbach, *Int. J. Hydrogen Energy*, 2002, **27**, 203-212.
6. B. Sakintuna, F. Lamari-Darkrim and M. Hirscher, *Int. J. Hydrogen Energy*, 2007, **32**, 1121-1140.
7. J. Huot, G. Liang and R. Schulz, *Applied Physics A: Materials Science & Processing*, 2001, **72**, 187-195.
8. L. J. Murray, M. Dinca and J. R. Long, *Chem. Soc. Rev.*, 2009, **38**, 1294-1314.
9. R. E. Morris and P. S. Wheatley, *Angew. Chem. Int. Ed.*, 2008, **47**, 4966-4981.
10. K. M. Thomas, *Catal. Today*, 2007, **120**, 389-398.
11. D. J. Collins and H.-C. Zhou, *J. Mater. Chem.*, 2007, **17**, 3154-3160.
12. J. L. C. Rowsell, A. R. Millward, K. S. Park and O. M. Yaghi, *J. Am. Chem. Soc.*, 2004, **126**, 5666-5667.
13. N. L. Rosi, J. Eckert, M. Eddaoudi, D. T. Vodak, J. Kim, M. O'Keeffe and O. M. Yaghi, *Science*, 2003, **300**, 1127-1129.
14. H. Cheng, L. Chen, A. C. Cooper, X. Sha and G. P. Pez, *Energy Environ. Sci.*, 2008, **1**, 338-354.
15. M. Dincă, A. Dailly, Y. Liu, C. M. Brown, D. A. Neumann and J. R. Long, *J. Am. Chem. Soc.*, 2006, **128**, 16876-16883.
16. M. Dincă and J. R. Long, *Angew. Chem. Int. Ed.*, 2008, **47**, 6766-6779.
17. J. G. Vitillo, L. Regli, S. Chavan, G. Ricchiardi, G. Spoto, P. D. C. Dietzel, S. Bordiga and A. Zecchina, *J. Am. Chem. Soc.*, 2008, **130**, 8386-8396.
18. H. Cheng, X. Sha, L. Chen, A. C. Cooper, M.-L. Foo, G. C. Lau, W. H. Bailey Iii and G. P. Pez, *J. Am. Chem. Soc.*, 2009, **131**, 17732-17733.
19. D. Zhao, D. Yuan and H.-C. Zhou, *Energy Environ. Sci.*, 2008, **1**, 222-235.
20. A. Hamaed, M. Trudeau and D. M. Antonelli, *J. Am. Chem. Soc.*, 2008, **130**, 6992-6999.
21. T. K. A. Hoang, A. Hamaed, G. Moula, R. Aroca, M. Trudeau and D. M. Antonelli, *J. Am. Chem. Soc.*, 2011, **133**, 4955-4964.
22. T. K. A. Hoang, L. Morris, J. M. Rawson, M. L. Trudeau and D. M. Antonelli, *Chem. Mater.*, 2012, **24**, 1629-1638.
23. M. Dincă, W. S. Han, Y. Liu, A. Dailly, C. M. Brown and J. R. Long, *Angew. Chem. Int. Ed.*, 2007, **46**, 1419-1422.
24. P. D. C. Dietzel, B. Panella, M. Hirscher, R. Blom and H. Fjellvag, *Chem. Commun.*, 2006, **0**, 959-961.
25. H. R. Moon, N. Kobayashi and M. P. Suh, *Inorg. Chem.*, 2006, **45**, 8672-8676.
26. K. Pareek, Q. Zhang, R. Rohan and H. Cheng, *Journal of Materials Chemistry A*, 2014, 10.1039/C1034TA01364F.
27. M. Dincă and J. R. Long, *J. Am. Chem. Soc.*, 2007, **129**, 11172-11176.
28. Y.-H. Kim, Y. Zhao, A. Williamson, M. J. Heben and S. B. Zhang, *Physical Review Letters*, 2006, **96**, 016102.
29. S. Gupta, S. Sharma and A. K. Narula, *J. Organomet. Chem.*, 1993, **452**, 1-4.
30. P. N. Kapoor, A. K. Bhagi, H. K. Sharma and R. N. Kapoor, *J. Organomet. Chem.*, 1989, **369**, 281-284.
31. H. Bonadeo and E. Silberman, *J. Mol. Spectrosc.*, 1969, **32**, 214-221.
32. T. Hatanaka, R. Miyake, Y. Ishida and H. Kawaguchi, *J. Organomet. Chem.*, 2011, **696**, 4046-4050.
33. P. Parilla, *http://www.hydrogen.energy.gov/pdfs/review12/st014_parilla_2012_o.pdf*, **Hydrogen Sorbent Measurement Qualification and Characterization**
34. K. Kaneko and K. Murata, *Adsorption*, 1997, **3**, 197-208.

35. T. K. A. Hoang, L. Morris, J. Sun, M. L. Trudeau and D. M. Antonelli, *Journal of Materials Chemistry A*, 2013, **1**, 1947-1951.
36. A. Hamaed, T. K. A. Hoang, G. Moula, R. Aroca, M. L. Trudeau and D. M. Antonelli, *J. Am. Chem. Soc.*, 2011, **133**, 15434-15443.
37. X. Hu, B. O. Skadtchenko, M. Trudeau and D. M. Antonelli, *J. Am. Chem. Soc.*, 2006, **128**, 11740-11741.
38. J. R. Holst, A. Trewin and A. I. Cooper, *Nat Chem*, 2010, **2**, 915-920.
39. Y. Zhang, G. Xu, Y. Sun, B. Han, T. B. W. T, Z. Chen, R. Rohan and H. Cheng, *RSC Advances*, 2013, **3**, 14934-14937.
40. T. K. A. Hoang, M. I. Webb, H. V. Mai, A. Hamaed, C. J. Walsby, M. Trudeau and D. M. Antonelli, *J. Am. Chem. Soc.*, 2010, **132**, 11792-11798.
41. T. K. Kim and M. P. Suh, *Chem. Commun.*, 2011, **47**, 4258-4260.
42. D. Yuan, D. Zhao, D. Sun and H.-C. Zhou, *Angew. Chem. Int. Ed.*, 2010, **49**, 5357-5361.
43. K. Sumida, C. M. Brown, Z. R. Herm, S. Chavan, S. Bordiga and J. R. Long, *Chem. Commun.*, 2011, **47**, 1157-1159.
44. X. Liu, M. Oh and M. S. Lah, *Inorg. Chem.*, 2011, **50**, 5044-5053.
45. T. K. Prasad, D. H. Hong and M. P. Suh, *Chemistry – A European Journal*, 2010, **16**, 14043-14050.
46. P. M. Budd, B. Ghanem, K. Msayib, N. B. McKeown and C. Tattershall, *J. Mater. Chem.*, 2003, **13**, 2721-2726.
47. X. Lin, I. Telepeni, A. J. Blake, A. Dailly, C. M. Brown, J. M. Simmons, M. Zoppi, G. S. Walker, K. M. Thomas, T. J. Mays, P. Hubberstey, N. R. Champness and M. Schröder, *J. Am. Chem. Soc.*, 2009, **131**, 2159-2171.

